We thank the two anonymous reviewers for their careful reading and constructive suggestions on the manuscript. Below, we explain how the comments and suggestions are addressed and make note of the revisions in the revised manuscript. The reviewers' comments are in blue color. Our replies are in black, and our corresponding revisions in the manuscript are in red.

Responses to reviewer #2

Shi et al. present a global modeling study to estimate the contribution of dust emitted at high latitudes as source of ice nucleating particles in the Arctic. They added a source tagging technique for dust from different regions to accomplish this. The role of dust in the climate system is an important topic, especially in high latitudes, which are experiencing a rapid change in climate. The paper makes an important contribution to this topic, since high-latitude dust contributions are largely unknown. At the same time the paper highlights several challenges -- simulating the global distribution of dust itself, but also estimating the concentration of ice nucleating particles based on the simulated dust distribution. The paper fits well within the scope of ACP, and I recommend the paper to be published after the following comments are addressed:

Reply: We thank the reviewer for the constructive comments, which have improved the quality of our manuscript. We have revised the manuscript following your comments.

1. Line 124: More detail is needed to describe the ice-nucleation parameterization that is used in the simulations (I believe this is the soccer-ball model?). How is dust represented using this parameterization? Are the same model parameters applied not matter from which region the dust comes from (i.e. different mineralogical composition is ignored)?

Reply: The ice nucleation parameterization used in the simulations is the classical nucleation theory (CNT) parameterization. Wang et al. (2014) implemented the CNT parameterization based on Hoose et al. (2010) into the Community Atmosphere Model (CAM) but improved it by using a probability density function (PDF) of contact angles for immersion freezing of dust instead of a single contact angle. In addition, CNT treats the deposition and contact ice nucleation on dust particles. Please note this scheme is not the soccer-ball model implemented by Wang and Liu (2014). Dust particles originated from different sources are treated the same in the model (i.e., the same PDF of contact angles used). We do not consider the differences in mineralogical composition. We provide more details about the CNT parameterization in Text S2.1. Please see more details in our responses to your comment #4.

2. Related to this, in section 3.3, different ice-nucleation parameterizations are used for the comparison with measurements. It seems that the default parameterization should be part of this comparison. I suggest adding this to this section.

Reply: Thanks for the suggestion. We agree with you on this. The default CNT parameterization is now included in the INP comparison in Section 3.3. We also revised Figure 8 accordingly. Overall, the results from the CNT comparison (new Figures 8a-8c) are consistent with those from the comparison of other dust ice nucleation parameterizations (new Figures 8d-8f) – including the contribution from HLD improves the model performance in simulating Arctic INP concentrations. The CNT parameterization produces 5 to 10 times higher INP concentrations than the other two schemes (D15 and SM20) at moderately cold temperatures (-22 to -28°C), while it has a significant underprediction of INP concentration at warm temperatures (T > -18°C).

The revised Figure 8 looks as follow.

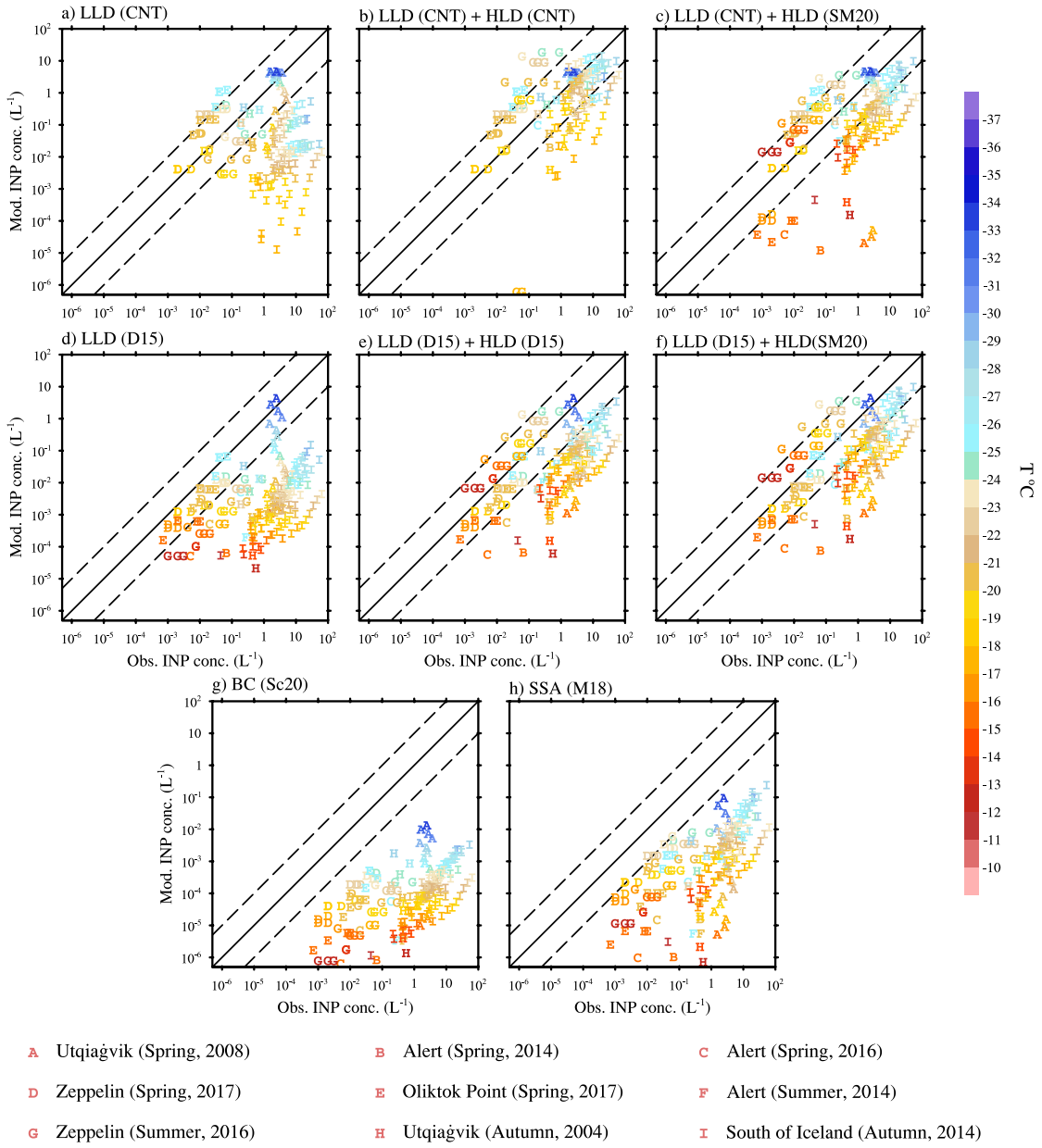

Figure 8. Comparison of predicted versus observed INP concentrations in the Arctic. The predicted INP concentrations are derived from a) LLD using classical nucleation theory (CNT), b) LLD and HLD, both using CNT, c) LLD using CNT and HLD using Sanchez-Marroquin et al (2020; SM20), c) LLD using DeMott et al. (2015; D15), d) LLD and HLD, both using D15, e) LLD using D15 and HLD using SM20, f) BC using Schill et al. (2020; Sc20), and g) SSA using McCluskey et al. (2018; M18). SSA includes both marine organic aerosol and sea salt. Nine INP datasets are classified by symbol "A" to "I", the color of which represents the temperature reported in the observations. The observations for datasets "A", "C", "E", "H" are monthly mean values. Samples for datasets "D", "G", "I" are selected randomly and only 15% of them are plotted. Details of each campaign are summarized in Table 3. The modelled INP concentrations are diagnosed using the observed temperatures and monthly averaged aerosol properties of the corresponding month from year 2007 to 2011. The INP concentrations for CNT are defined as the CNT immersion freezing rate integrated by 10 s, following Hoose et al. (2010) and Wang et al. (2014). Solid line in each panel represents 1:1 comparison, while dashed lines outline one order of magnitude differences. The unit for INP concentration is L^{-1}.

We added a brief discussion regarding CNT in Section 3.3:

Line 395-401: "Overall, only including LLD as INPs results in up to four orders of magnitude underprediction compared to observations (Figure 8a and 8d), while taking into account the contribution from HLD greatly improves the model performance by increasing the simulated dust INP concentrations (Figures 8b, 8c, 8e, and 8f). The CNT parameterization produces 5 to 10 times more INP concentrations than the other two schemes at moderately cold temperatures (-22 to -28 ℃), while it has a significant underestimation of observed INP concentrations at warm temperatures (T > -18℃) (also see Figure S4)."

We also added a new figure (new Figure S4) in the supporting information showing the relationship of simulated INP concentrations and the temperatures. The new Figure S4 looks as follow.

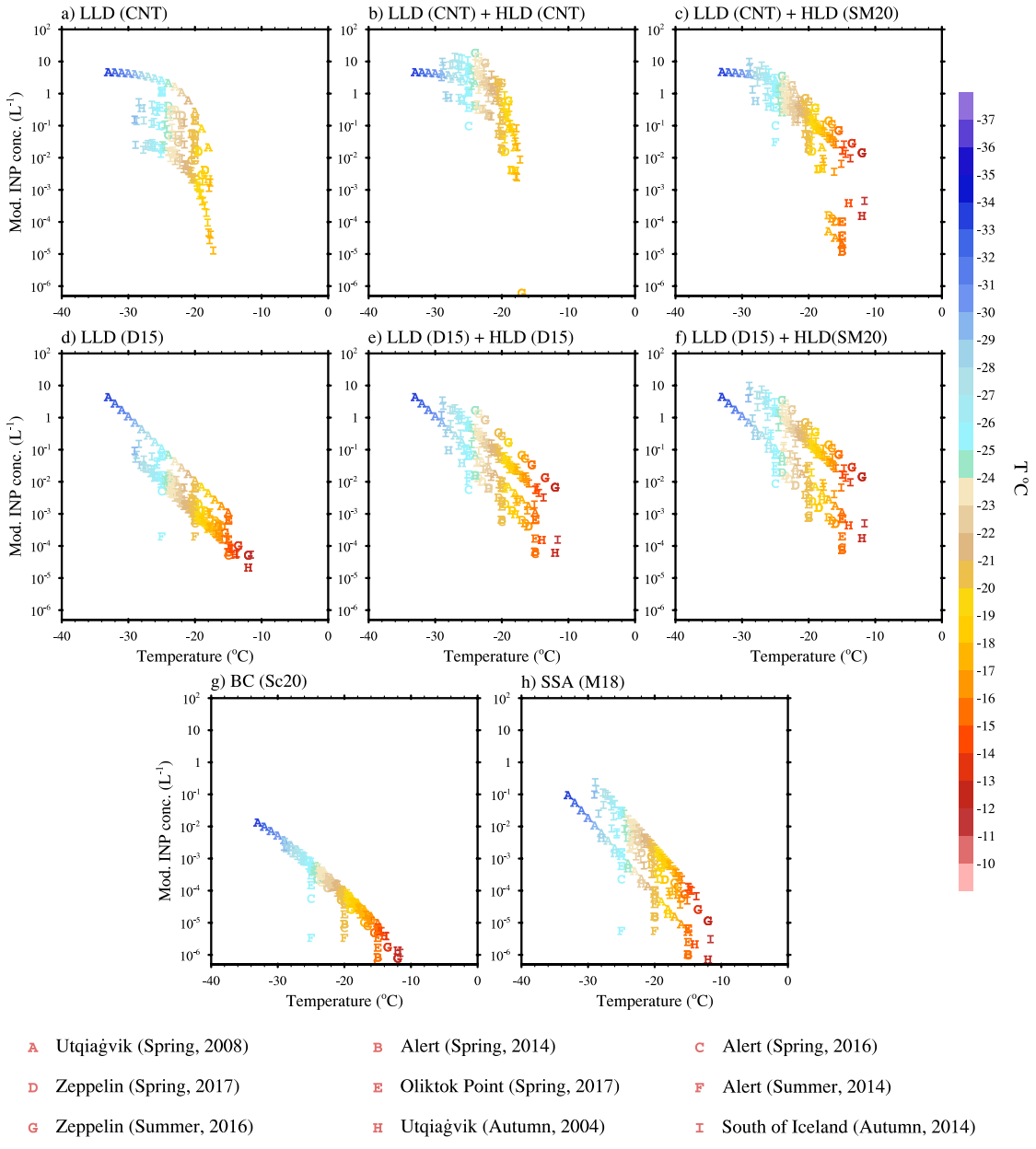

Figure S4. Simulated INP concentrations as a function of temperature. The simulated INP concentrations are derived from a) LLD using classical nucleation theory (CNT), b) LLD and HLD, both using CNT, c) LLD using CNT and HLD using Sanchez-Marroquin et al (2020; SM20), c) LLD using DeMott et al. (2015; D15), d) LLD and HLD, both using D15, e) LLD using D15 and HLD using SM20, f) BC using Schill et al. (2020; Sc20), and g) SSA using McCluskey et al. (2018; M18). The temperature of each data point is also shown by its color. Nine INP datasets are classified by symbol "A" to "I". This figure is based on the same simulated INP concentrations that used from Figure 8.

3. Line 134: What was the rational for choosing the time period 2006 to 2011? (and not for example a more recent time period for example)

Reply: The primary reason for choosing year 2007 to 2009 is to match the time period for the CALIPSO dust retrievals (Luo et al., 2015a, b). We regard the CALIPSO dust extinction as a very valuable dataset because it gives vertical profiles for almost the entire Arctic region. We then extended the simulations to year 2011 to reduce noises that shows up in the dust INP effects. Also, we have tuned the global dust optical depth to 0.030±0.005, which is based on the estimates by Ridley et al. (2016) over year 2004-2008. Therefore, considering the possible decadal changes in global dust distribution, a second reason for choosing this time period (not a more recent one) is that we want the simulations to be conducted in a time period that is closer to that from Ridley et al. (2016).

We note that choosing this time period leads to biases in comparing our model results with measurements conducted in other time periods. This may be particularly true for the INP comparisons, because 7 out of 9 INP datasets we use were conducted after year 2012 and the year-to-year variability may be large for the measured INPs in the Arctic. However, considering the large uncertainties with the INPs, this year-to-year variability is of secondary order.

4. Line 150: Similar to comment 1, I recommend explaining more detail (i.e. equations) about the dust emission parameterization as well as the source tagging procedure. INP parameterization, dust emission parameterization and source tagging are central to this paper, so even though they are described in other papers, it will be helpful for the reader to have the information easily available. This could go in an Appendix or even the SI.

Reply: Thanks for the suggestion. The source tagging procedure is implemented by assigning dust emitted from different sources to separate tracers. It does not involve changes in equations. We add a few sentences to explain the implementation of the source-tagging technique in the revised manuscript:

Line 167-170: "In this method, dust emission fluxes from different sources are assigned to separate tracers and transport independently, so that dust originating from different sources can be tracked and tuned separately in a single model experiment."

We provide equations for the dust emission parameterization and ice nucleation parameterizations in the revised SI (Text S1 and S2):

"**Text S1: K14 dust emission parameterization**

Kok et al. (2014a, b) (K14) is a physically based dust emission scheme that removes the need to use an empirical dust soil erodibility map in other parameterizations (e.g., Zender et al., 2003). The vertical dust emission flux, F_d (kg m^{-2} s^{-1}) is given by

$$F_d = C_d f_{bare} f_{clay} \frac{\rho_a(u_*^2 - u_{*t}^2)}{u_{*st}} \left(\frac{u_*}{u_{*t}}\right)^{C_\alpha \frac{u_{*st}-u_{*st0}}{u_{*st0}}}, (u_* > u_{*t}), \quad \text{(S1)}$$

where C_d is the dimensionless dust emission coefficient, f_{bare} is the fraction of the surface consisting of bare soil, f_{clay} is the soil clay fraction, ρ_a (kg m^{-3}) is the air density, u_* (m s^{-1}) is the soil friction velocity, u_{*t} (m s^{-1}) is the threshold of soil friction velocity above which saltation occurs, u_{*st} (m s^{-1}) is the soil threshold friction velocity standardized to standard atmospheric density, u_{*st0} (m s^{-1}) is the standardized threshold friction velocity of an optimally erodible soil, and C_α is the dimensionless constant scaling the fragmentation exponent (α).

Text S2: Ice nucleation parameterizations

In this section, we introduced five ice nucleation parameterizations used in this study. They can be classified into two types: the stochastic approach, which treats ice nucleation as a time-dependent process, and the deterministic approach, which assumes that ice nucleation is time-invariant and only depends on temperature and aerosol properties. In this study, the CNT parameterization follows the stochastic approach, while the other four parameterizations follow the deterministic approach.

S2.1 CNT parameterization

The classical nucleation theory (CNT) scheme is used for heterogeneous ice nucleation in mixed-phase clouds in EAMv1 simulations. This parameterization was first implemented in a global climate model by Hoose et al. (2010), and further improved by Wang et al. (2014) by introducing a probability density function of contact angles (α-PDF) for immersion freezing of natural dust. In CNT, immersion/condensation, contact, and deposition nucleation on dust and BC are treated. The rate of heterogeneous nucleation per aerosol particle and time, J_{het}, is expressed by

$$J_{het} = \frac{A' r_N^2}{\sqrt{f}} \exp\left(\frac{-\Delta g^\# - f \Delta g_g^o}{kT}\right), \quad \text{(S2)}$$

where A' is a prefactor, r_N is the aerosol particle radius, f is a form factor describing the aerosol's ice nucleating ability, $\Delta g^\#$ is the activation energy, Δg_g^o is the homogeneous energy of germ formation, k is the Boltzmann constant, and T is the temperature in K. The factor, f, is a function of contact angle, α, in the form,

$$f = \frac{1}{4}(2+m)(1-m)^2, \quad \text{(S3)}$$

where $m \equiv cos\alpha$. The contact angle is assumed to follow a log-normal distribution in the form,

$$p(\alpha) = \frac{1}{\alpha\sigma\sqrt{2\pi}} \exp\left(-\frac{(\ln(\alpha) - \ln(\mu))^2}{2\sigma^2}\right), \quad \text{(S4)}$$

where μ is the mean contact angle and σ is the standard deviation.

We do not consider the differences in the mineralogical composition in different dust sources. Thus, dust particles originated from different sources are treated the same in the CNT (i.e., same contact angle distribution). The parameterization considers the immersion freezing point depression by coating of sulfate aerosols (Hoose et al., 2010). However, this effect has no

differences for HLD and LLD, because aerosol species (e.g, dust, sulfate) are assumed to be internally mixed within an aerosol mode in the MAM4 aerosol module (Liu et al., 2016).

S2.2 D15 parameterization

The DeMott et al. (2015; D15) parameterization is a dust immersion freezing ice nucleation parameterization derived from a combination of laboratory and field data. The laboratory data are from ice nucleation experiments on Saharan and Asian desert dust using the Aerosol Interaction and Dynamics in the Atmosphere chamber. The field data were collected over the Pacific Ocean basin and US Virgin Islands, which are dominated by Asian and Saharan desert dust, respectively. Thereby, D15 can be regarded as a LLD ice nucleation parameterization in our study, though it is also applied to HLD in Figure 8f for sensitivity studies. In D15, dust INP number concentration, n_{INP} (std L^{-1}), is related to temperature, T_k (K), and the number concentration of dust particles larger than 0.5 μm, $n_{a>0.5\mu m}$ (std cm^{-3}), in the form,

$$n_{INP}(T_k) = (cf)(n_{a>0.5\mu m})^{\alpha(273.16-T_k)+\beta} \exp\left(\gamma(273.16 - T_k) + \delta\right), \quad \text{(S5)}$$

where cf = 3, α = 0, β = 1.25, γ = 0.46, and δ = -11.6.

S2.3 SM20 parameterization

The Sanchez-Marroquin et al. (2020; SM20) parameterization is based on aircraft-collected freshly emitted Icelandic dust samples and thus is treated as a parameterization for HLD in our study. It is an immersion freezing ice nucleation scheme formulated in terms of the ice-nucleating active surface site density (INAS). The total INP concentration, n_{INP} (L^{-1}), is given by

$$n_{INP} = n_{HLD}\{1 - \exp\left[-S_{ae}n_s\right]\}, \quad \text{(S6)}$$

where n_{HLD} (L^{-1}) is the number concentration of HLD, S_{ae} (m^2) is the surface area of a single HLD particle, and n_s (m^{-2}) is the density of active sites. n_s is in the form

$$n_s(T) = 10^{-0.0337-0.199T}, \quad \text{(S7)}$$

where T is temperature in °C.

S2.4 Sc20 parameterization

The Schill et al. (2020; Sc20) parameterization is an INAS-based immersion freezing ice nucleation parameterization based on smoke from western US wildfires and grassland prescribed burns. It is an ice nucleation parameterization for biomass burning black carbon (BC), but we apply it to BC from both biomass burning and fossil fuel combustion. The total INP concentration is given by the same equation as Eq.(S6), except n_{HLD} is replaced by n_{BC}, which is the number concentration of BC. The n_s fit for Sc20 is given by

$$n_s(T) = \exp(1.844 - 0.684T - 0.00597T^2), \quad \text{(S8)}$$

where T is temperature in °C.

S2.5 M18 parameterization

The McCluskey et al. (2018; M18) parameterization is an INAS based immersion freezing ice nucleation parameterization for sea spray aerosols (SSAs; includes sea salt and marine organic aerosol) derived from pristine marine air mass measurements at the Mace Head Research Station.

The total INP concentration is given by the same equation as Eq.(S6), except n_{HLD} is replaced by n_{SSA}, which is the number concentration of SSA. The n_s fit for M18 is given by

$$n_s(T_k) = \exp(-0.545(T_k - 273.15) + 1.0125), \quad \text{(S9)}$$

where T_k is temperature in K."

5. Line 155-157: Are the differences between the mass assignments to modes in Z03 and Kok (2011) significant?

Reply: Global models usually have large uncertainties in simulating dust. To add some constraints to the global dust fields, the global averaged dust optical depth (DOD) is usually tuned to be within the range of the observational estimate (0.030±0.005) by Ridley et al. (2016). This is what we did for our CTRL experiment and thus the global averaged DOD does not change much by changing the mass assignments.

When we change the mass assignments from Z03 to Kok (2011) by shifting dust mass from the accumulation mode to the coarse mode, we need to raise the global dust emission fluxes to match the global averaged DOD because the coarse mode dust contributes less to total DOD than the accumulation mode dust per mass base. Therefore, dust emission fluxes and dust burden both increase after changing the emission size distribution from Z03 to K11. We note the dust burden changes are more obvious near the dust sources, because the coarse dust particles are removed readily during transport. The remote regions (the Arctic) are less affected by changing the dust emission size distributions.

6. Explanation of quantities shown in the figures: Please add information in the caption over what time period the model results were averaged. For example, in Fig 3, is this the average over the entire simulated period (2006-2011)? If so, what is the year-to-year variability? And is it the same time period for the observations? What does the grey band represent?

Reply: In Figure 3, the model results are averaged from 2007 to 2011. It is not the same time period for the observations. We add the year-to-year variability of the modelled total dust concentration (the pink shade) to Figure 3. The grey band represents the standard deviation of observations. We revise Fig. 3 and its caption following your suggestions.

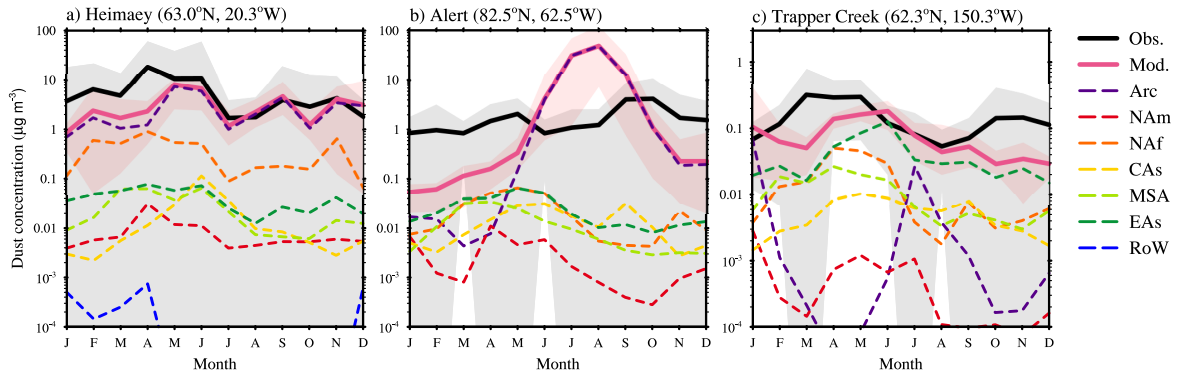

Figure 3. Comparison of measured (black solid line, with gray shade representing standard deviation) and simulated (pink solid line, with pink shade representing year-to-year variability) monthly mean dust surface concentration at three high latitude stations – a) Heimaey, b) Alert, and c) Trapper Creek. The model results are averaged from year 2007 to 2011. Contributions from seven tagged sources are shown by colored dashed lines. The locations of the three stations are shown in Figure 2d. The measurements at Heimaey (Prospero et al., 2012), Alert (Sirois and Barrie, 1999), and Trapper Creek (IMPROVE) are averaged for the years 1997 to 2002, 1980 to 1995, and 2007 to 2011, respectively. The dust concentrations at Trapper Creek only include particles with diameter less than 2.5 μm. The other two stations include dust over the whole size range.

7. Fig 4: The caption mentions that the model results were averaged w.r.t time (2007-2011) and space. I suggest showing some measure of variability, with respect to time and space, to be better able to judge the agreement with the observations.

Reply: Following your suggestion, we have added the standard deviation with respect to time and space for the simulated total dust concentrations on Fig. 4. The revised figure and figure caption looks as follow:

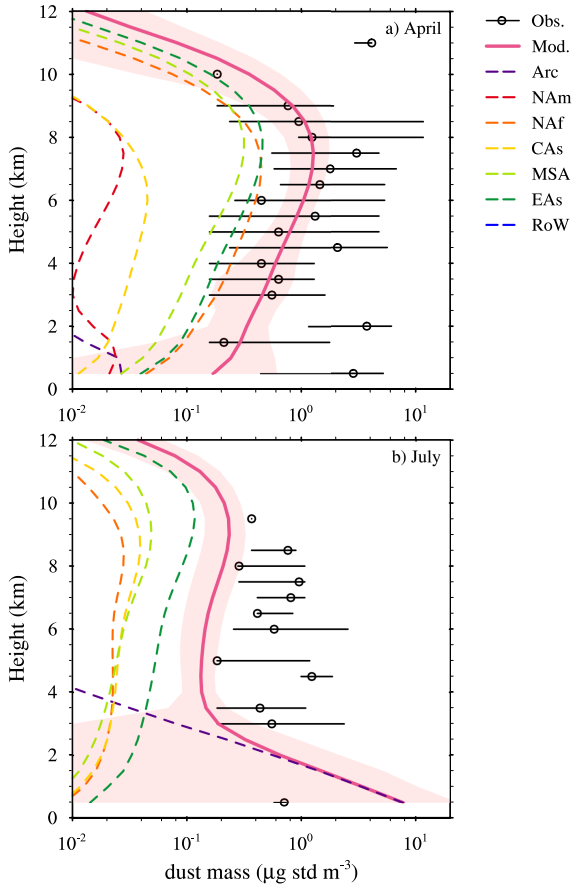

Figure 4. Comparison of vertical dust concentrations from ARCTAS flight observations (Jacob et al., 2010) (black circle) and CTRL simulation (pink solid line) in a) April and b) July. We show median values for observations at each level. The maximum and minimum of the measurements at each level are shown by black lines. Contributions from the seven tagged sources in CTRL are shown by colored dashed lines. The ARCTAS dust mass concentrations are derived from measured calcium and sodium concentrations. The measurements data are processed using the same method as Breider et al. (2020). Briefly, we assume a calcium to dust mass ratio of 6.8% and further correct the calcium concentrations for sea salt by assuming a calcium to sodium ratio of 4%. Only measurements obtained north of 60°N are used for the analyses. The low-altitude observations near Fairbanks, Barrow, and Prudhoe Bay are removed. Also, data from below 1 km on 1, 4, 5, 9 July is removed to exclude the influence of wildfire. The ARCTAS flight campaign was conducted in 2008, while the modeled vertical profiles are averaged for each April and July from 2007 to 2011, respectively. Following Groot Zwaaftink et al. (2016), the simulation profiles are averaged for the regions north of 60°N and 170°W to 35°W in April and 135°W to 35°W in July. The pink shade on each panel represents the standard deviation with respect to time and space for the simulated total dust concentrations.

8. Figs 5, 6, 7, 9, 10, 11, 12, 13: Include the time averaging interval in the captions.

Reply: Thanks for the suggestion. We have included the time averaging interval for model results in the captions of these figures. Briefly, only Figure 5 is averaged from 2007 to 2009 to match the

period of CALIPSO retrieval, while all the other figures are averaged over the entire simulation period (2007 to 2011).

9. Line 257: I would argue that also the MAM case is consistently underestimated by the model and that DJF is underestimated near the surface. However, this is difficult to judge because neither observations nor model results contain any measure of uncertainty. It may well be that the two actually agree within the level of uncertainty. Please include some discussion about this.

Reply: We added year-to-year variability of the simulated dust extinction results in Figure 5. The revised Figure 5 looks as follow.

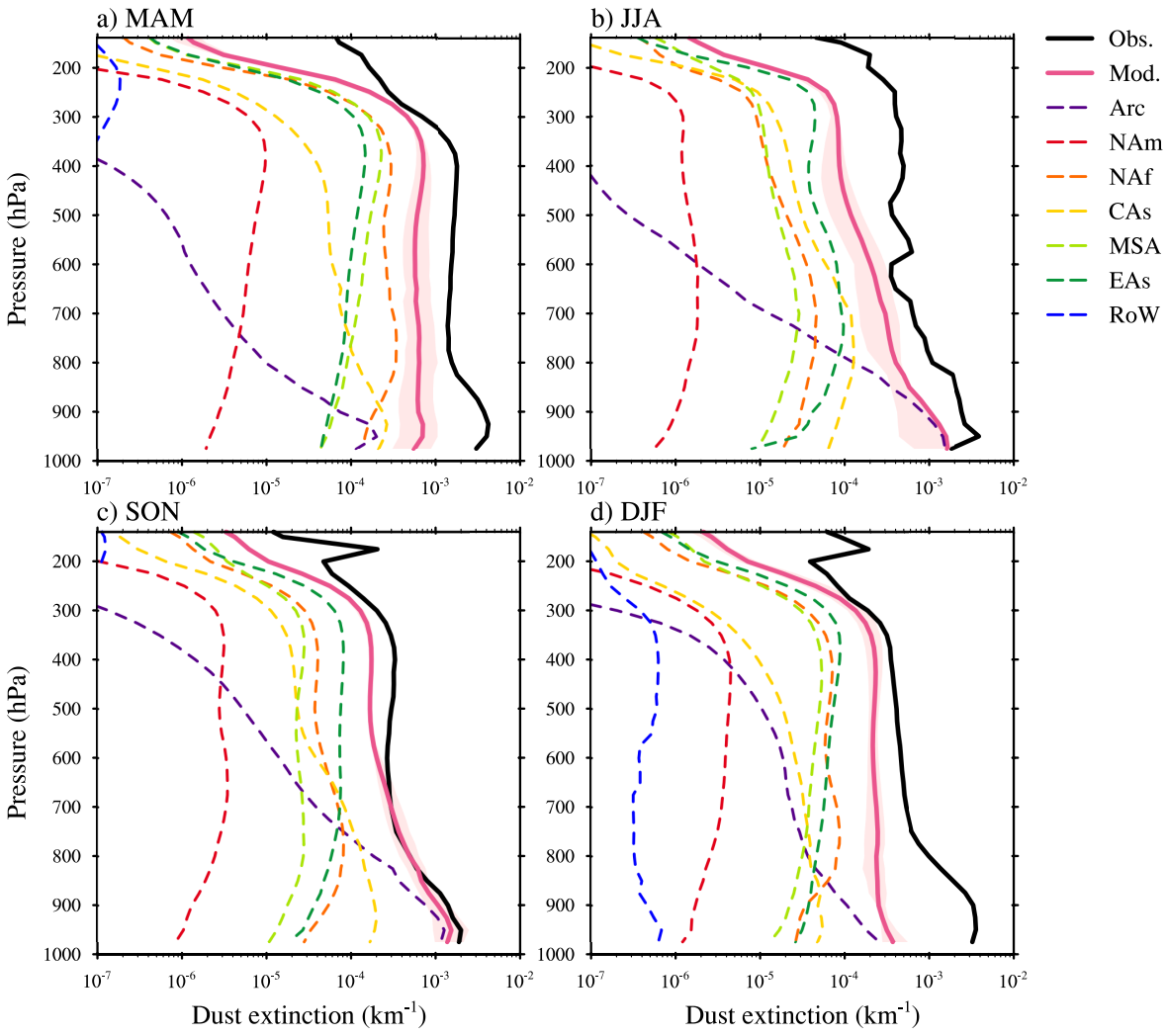

Figure 5. Comparison of seasonal CALIPSO retrieved (Luo et al., 2015a, b) (black solid line) and model simulated (pink solid line; with pink shade representing year-to-year variability) dust extinction vertical profiles in the Arctic. Contributions from seven tagged sources are shown by

colored dashed lines. The CALIPSO retrieval is for the year 2007 to 2009, while the model is averaged over the same years.

We agree with the reviewer on the consistent underestimation in MAM and the near surface underestimation in DJF. We add some discussions regarding these issues in Section 3.1:

Line 274-280: "The simulated dust extinction also shows a consistent underestimation in springtime (MAM) and a near surface underestimation in wintertime (DJF). Since the Arctic is mostly covered by ice and snow in these two seasons, the impacts of HLD are expected to be limited and the low biases are most likely due to the underprediction of LLD transport. The near surface underestimation in DJF may indicate a too weak LLD transport in the lower troposphere (e.g., the transport of dust emitted from Central Asia; see Figure 7 and the corresponding discussions in Section 3.2)."

10. Figure 6: It would be instructive to additionally represent this figure with percentage contributions rather with absolute values for the column burden. This would make it easier to convey the information how much each region contributes to the burden in a given location.

Reply: We have added the spatial distribution of percentage contributions from each source to the annual mean dust column burden in the supplementary (new Figure S2). The new figure looks as follow.

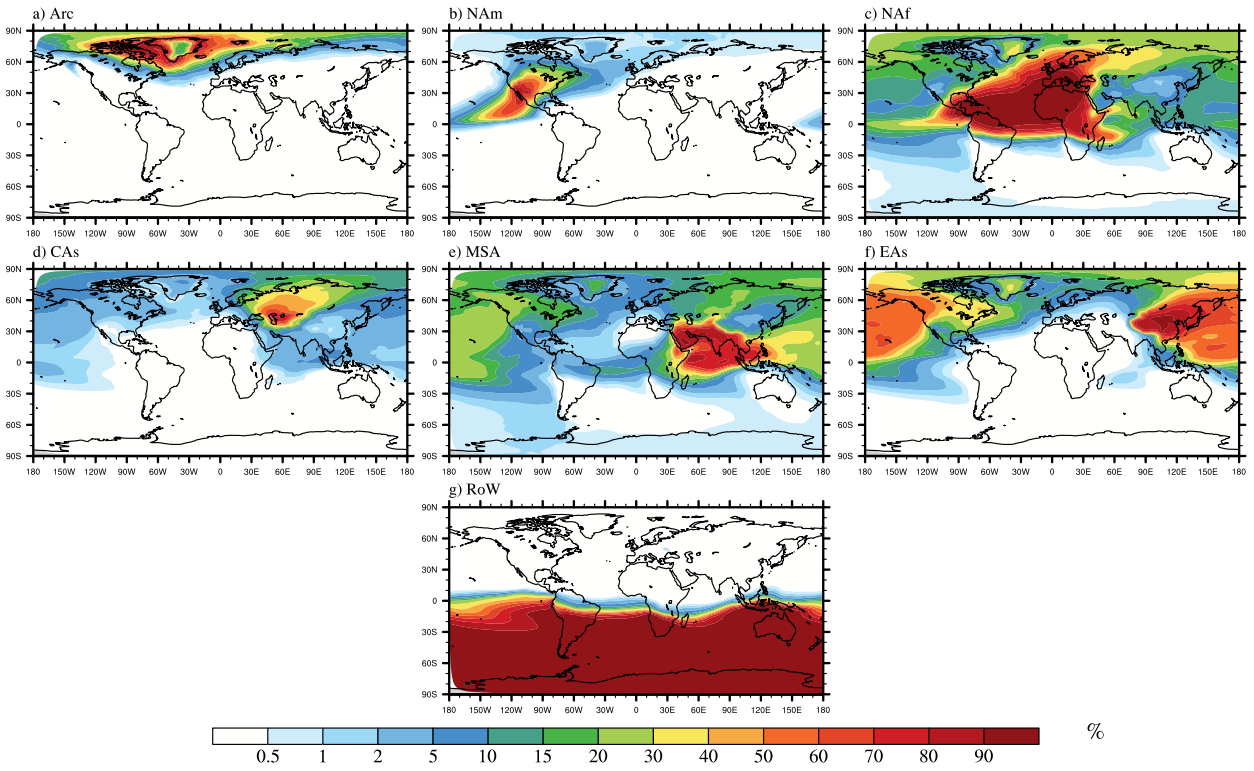

Figure S2. Global distribution of relative contributions (%) to the annual mean (2007 to 2011) dust column burden from each tagged source region.

We also added/modified some descriptions/discussions about the new Figure in the revised Section 3.2:

Line 287-289: "The transport pathways can be identified from the dust burden spatial distribution for each source in Figure 6, while the relative contribution of each source to the total dust burden is shown in Figure S2."

Line 295-299: "As shown in Figure 6a and Figure S2a, the local dust is confined within the high latitudes, with the higher amounts and higher contributions to the total dust burden near the sources in North Canada, coast of Greenland, and Iceland. The interior of the Greenland ice sheet, with its higher elevations, is more influenced by LLD from North Africa and East Asia than HLD (Figure S2c and S2f)."

Line 320-321: "Overall, the LLD from North Africa and Asia contributes more to the Eurasia and Pacific sector of the Arctic (Figures S2c to S2f)."

11. Figure 8: Suggest adding quantity and unit (INP conc. / L^{-1}) as axes labels. How are the temperatures chosen – are they determined by what was used in the observations? How exactly were the time intervals of observations and measurements matched up? Line 346 mentions "monthly averaged aerosol populations" while Table 3 only lists Spring/Summer/Autumn of various years.

Reply: We have changed the axes labels of Figure 8 to "Mod. INP conc. (L^{-1})" and "Obs. INP conc. (L^{-1})" following your suggestion. As you mentioned, the temperatures we used are determined by what was reported in the INP measurements. We did not intentionally do any average for the observation data we have. However, depending on the data availability, the data we have may already be processed to monthly averages (datasets A, C, E, H in Table 3). Also, some of the datasets (datasets D, G, I) have too many samples to be plotted clearly. To improve the presentation of the figure, we randomly select 15% of the data points in these datasets to plot (we did not take average). We have confirmed that the range of the selected samples is very close to the whole dataset. For each observed data point (i.e., each symbol on Figure 8), we used the model monthly averaged aerosol properties of the corresponding month from year 2007 to 2011 to diagnose the simulated INP concentrations. To clarify this, we added the exact months of the sampling period for each measurement in Table 3, column 3. The new Table 3 looks as follow.

Table 3. Summary of the nine Arctic INP measurements used for INP comparisons in Figure 8.

	Location	Time period	Measured platform	Reference	Possible INP source mentioned in literature	INP source attribution from modeling[+]
A	Utqiaġvik	Apr. 2008 (spring)	Aircraft	McFarquhar et al. (2011)	Metallic or composed of dust[*]	LLD (EAs)
B	Alert	Mar. - May 2014 (spring)	Ground-based	Mason et al. (2016)	Not mentioned	LLD (EAs)
C	Alert	Mar. 2016 (spring)	Ground-based	Si et al. (2019)	LLD from Gobi Desert	LLD (EAs)
D	Zeppelin	Mar. 2017 (spring)	Ground-based	Tobo et al. (2019)	Marine organic aerosols	HLD (NEu)
E	Oliktok Point	Mar. - May 2017 (spring)	Ground-based	Creamean et al. (2018)	Dust and primary marine aerosols	LLD (mainly from EAs and some from NAf)
F	Alert	Jun. - Jul. 2014 (summer)	Ground-based	Mason et al. (2016)	Not mentioned	HLD (NCa)
G	Zeppelin	Jul. 2016 (summer)	Ground-based	Tobo et al. (2019)	HLD from Svalbard or other high latitude sources[**]	HLD (NEu)
H	Utqiaġvik	Oct. 2004 (autumn)	Aircraft	Prenni et al. (2007)	Dust and carbonaceous particles	HLD (NCa) and LLD (EAs)
I	South of Iceland	Oct. 2014 (autumn)	Aircraft	Sanchez-Marroquin et al. (2020)	Icelandic dust	Dominated by HLD (GrI), little from LLD (NAf)

[+] The modeling analyses include INP contribution from HLD (using SM20), LLD (using D15), BC, and SSA.
[*] Carbonate, black carbon, and organic may also contribute, according to Hiranuma et al. (2013).
[**] The HLD in this campaign is reported to have remarkably high ice nucleating ability, which may be related to the presence of organic matter.

12. Section 3.3: there are various INP parameterizations out there for various kinds of dust. While I don't expect the authors to compare all of them, I suggest discussing the reason for the choices made for this paper since the choice of the parameterization can have a big impact on the result. (However, I do recommend including the default parameterization, see comment 2 above).

Reply: We use D15 for the LLD INP because it produced the most reasonable LLD INP concentrations in EAMv1 based on our earlier study (Shi and Liu, 2019). There are various other LLD INP parameterizations, many of which are based on the ice-nucleating active surface site density (INAS) (e.g., Niemand et al., 2012; Ullrich et al., 2017). The Niemand et al. (2012) parameterization was tested in Shi and Liu (2019), which concluded that Niemand et al. (2012) may have an overestimation of Arctic INP concentrations in EAMv1, which is likely because the simulated aerosol size distribution in the Arctic is biased to the small size range. We expect the other INAS-based schemes to produce a similar results to Niemand et al. (2012). So, we do not use them in our current study. There are also INP parameterizations based on dust minerology (e.g., Atkinson et al., 2013; Harrison et al., 2019), which are not used because we do not represent dust speciation in the current model.

There are not a lot of HLD INP parameterizations (or even data) as compared to LLD INP parameterizations. To our knowledge, Paramonov et al. (2018) analyze the ice nucleation ability of soil samples collected from Iceland and provide an INAS-based fit. We use the SM20 parameterization which was developed based on airborne samples rather than Paramonov et al. (2018) in our study, due to the possible large ice nucleation ability differences between soil samples and airborne dust samples.

Please see our reply to your comment 2 above, we have included the default CNT parameterization in the mode-observation INP comparison.

We add a section in Text S2 in the supporting information to discuss the choice of the dust parameterizations.

"**S2.6 Discussion regarding the choice of dust ice nucleation parameterizations**

In this study, we use three dust ice nucleation parameterizations (i.e., CNT, D15, and SM20). CNT is chosen because it is the default ice nucleation scheme for EAMv1. We use D15 because it is found to produce the most reasonable INP concentrations in EAMv1 based on our earlier study (Shi and Liu, 2019). There are various other LLD INP parameterizations, many of which are INAS-based (e.g., Niemand et al., 2012; Ullrich et al., 2017). The Niemand et al. (2012) parameterization was tested in Shi and Liu (2019) and was found to overestimate the Arctic INP concentrations with corrected dust concentrations in EAMv1. There are also INP parameterizations based on dust minerology (e.g., Atkinson et al., 2013; Harrison et al., 2019), which are not used because we do

not represent dust speciation in the current model. There are not a lot of HLD INP parameterizations (or even data) as compared to LLD INP schemes. To our knowledge, Paramonov et al. (2018) analyze the ice nucleation ability of soil samples collected from Iceland and provide an INAS-based fit. We use SM20 which was developed based on airborne samples rather than Paramonov et al. (2018) in our study, due to the possible large differences between soil samples and airborne dust samples."

13. Code availability: The github link only points to the general E3SM repo. The authors should include the code that was actually used to run the simulations (including the tagging), for example using zenodo archiving: https://guides.github.com/activities/citable-code/

Reply: This work is funded by the Department of Energy (DOE) Atmospheric System Research (ASR) Program. Unfortunately, we cannot share the code without the permission from DOE.

Typographical errors:

1. Line 126: Explain WBF

Reply: The WBF process has been explained in the revised manuscript:

Line 38-42: "The AMPCs lifetime, properties, and radiative effects are closely connected to the primary ice formation process, as the formed ice crystals grow at the expense of cloud liquid droplets due to the lower saturation vapor pressure with respect to ice than that to liquid water (so-called Wegener-Bergeron-Findeisen process or, in short, WBF process; Liu et al., 2011; M. Zhang et al., 2019)."

2. Line 133: Should read "are shown"

Reply: It has been corrected. Thanks.

General comment: Axes labels: I recommend to not use the format 1E-6 etc. to represent numbers, but use 10^{-6} etc. instead.

Reply: We updated Figs. 1, 2, 3, 6, 8, S1 and S8 following your suggestion.

Reference

Albani, S., Mahowald, N. M., Perry, A. T., Scanza, R. A., Zender, C. S., Heavens, N. G., Maggi, V., Kok, J. F., and Otto-Bliesner, B. L.: Improved dust representation in the Community Atmosphere Model, J. Adv. Model. Earth Syst., 6, 541–570, https://doi.org/10.1002/2013MS000279, 2014.

Atkinson, J. D., Murray, B. J., Woodhouse, M. T., Whale, T. F., Baustian, K. J., Carslaw, K. S., Dobbie, S., O'Sullivan, D., and Malkin, T. L.: The importance of feldspar for ice nucleation by mineral dust in mixed-phase clouds, Nature, 498, 355–358, https://doi.org/10.1038/nature12278, 2013.

Boose, Y., Sierau, B., García, M. I., Rodríguez, S., Alastuey, A., Linke, C., Schnaiter, M., Kupiszewski, P., Kanji, Z. A., and Lohmann, U.: Ice nucleating particles in the Saharan Air Layer, Atmos. Chem. Phys., 16, 9067–9087, https://doi.org/10.5194/acp-16-9067-2016, 2016.

DeMott, P. J., Prenni, A. J., McMeeking, G. R., Sullivan, R. C., Petters, M. D., Tobo, Y., Niemand, M., Möhler, O., Snider, J. R., Wang, Z., and Kreidenweis, S. M.: Integrating laboratory and field data to quantify the immersion freezing ice nucleation activity of mineral dust particles, Atmos. Chem. Phys., 15, 393–409, https://doi.org/10.5194/acp-15-393-2015, 2015.

Fan, S.-M.: Modeling of observed mineral dust aerosols in the arctic and the impact on winter season low-level clouds: DUST AND LOW-LEVEL CLOUDS IN THE ARCTIC, J. Geophys. Res. Atmos., 118, 11,161-11,174, https://doi.org/10.1002/jgrd.50842, 2013.

Harrison, A. D., Lever, K., Sanchez-Marroquin, A., Holden, M. A., Whale, T. F., Tarn, M. D., McQuaid, J. B., and Murray, B. J.: The ice-nucleating ability of quartz immersed in water and its atmospheric importance compared to K-feldspar, 19, 2019.

Hoose, C., Kristjánsson, J. E., Chen, J.-P., and Hazra, A.: A Classical-Theory-Based Parameterization of Heterogeneous Ice Nucleation by Mineral Dust, Soot, and Biological Particles in a Global Climate Model, 67, 2483–2503, https://doi.org/10.1175/2010JAS3425.1, 2010.

Huneeus, N., Schulz, M., Balkanski, Y., Griesfeller, J., Prospero, J., Kinne, S., Bauer, S., Boucher, O., Chin, M., Dentener, F., Diehl, T., Easter, R., Fillmore, D., Ghan, S., Ginoux, P., Grini, A., Horowitz, L., Koch, D., Krol, M. C., Landing, W., Liu, X., Mahowald, N., Miller, R., Morcrette, J.-J., Myhre, G., Penner, J., Perlwitz, J., Stier, P., Takemura, T., and Zender, C. S.: Global dust model intercomparison in AeroCom phase I, Atmos. Chem. Phys., 11, 7781–7816, https://doi.org/10.5194/acp-11-7781-2011, 2011.

Kok, J. F.: A scaling theory for the size distribution of emitted dust aerosols suggests climate models underestimate the size of the global dust cycle, Proceedings of the National Academy of Sciences, 108, 1016–1021, https://doi.org/10.1073/pnas.1014798108, 2011.

Kok, J. F., Mahowald, N. M., Fratini, G., Gillies, J. A., Ishizuka, M., Leys, J. F., Mikami, M., Park, M.-S., Park, S.-U., Van Pelt, R. S., and Zobeck, T. M.: An improved dust emission model –

Part 1: Model description and comparison against measurements, Atmos. Chem. Phys., 14, 13023–13041, https://doi.org/10.5194/acp-14-13023-2014, 2014a.

Kok, J. F., Albani, S., Mahowald, N. M., and Ward, D. S.: An improved dust emission model – Part 2: Evaluation in the Community Earth System Model, with implications for the use of dust source functions, Atmos. Chem. Phys., 14, 13043–13061, https://doi.org/10.5194/acp-14-13043-2014, 2014b.

Kulkarni, G., Sanders, C., Zhang, K., Liu, X., and Zhao, C.: Ice nucleation of bare and sulfuric acid-coated mineral dust particles and implication for cloud properties, 119, 9993–10011, https://doi.org/10.1002/2014JD021567, 2014.

Liu, X., Ma, P.-L., Wang, H., Tilmes, S., Singh, B., Easter, R. C., Ghan, S. J., and Rasch, P. J.: Description and evaluation of a new four-mode version of the Modal Aerosol Module (MAM4) within version 5.3 of the Community Atmosphere Model, Geosci. Model Dev., 9, 505–522, https://doi.org/10.5194/gmd-9-505-2016, 2016.

McCluskey, C. S., Ovadnevaite, J., Rinaldi, M., Atkinson, J., Belosi, F., Ceburnis, D., Marullo, S., Hill, T. C. J., Lohmann, U., Kanji, Z. A., O'Dowd, C., Kreidenweis, S. M., and DeMott, P. J.: Marine and Terrestrial Organic Ice-Nucleating Particles in Pristine Marine to Continentally Influenced Northeast Atlantic Air Masses, J. Geophys. Res. Atmos., 123, 6196–6212, https://doi.org/10.1029/2017JD028033, 2018.

Niemand, M., Möhler, O., Vogel, B., Vogel, H., Hoose, C., Connolly, P., Klein, H., Bingemer, H., DeMott, P., Skrotzki, J., and Leisner, T.: A Particle-Surface-Area-Based Parameterization of Immersion Freezing on Desert Dust Particles, 69, 3077–3092, https://doi.org/10.1175/JAS-D-11-0249.1, 2012.

Paramonov, M., David, R. O., Kretzschmar, R., and Kanji, Z. A.: A laboratory investigation of the ice nucleation efficiency of three types of mineral and soil dust, Atmos. Chem. Phys., 18, 16515–16536, https://doi.org/10.5194/acp-18-16515-2018, 2018.

Ridley, D. A., Heald, C. L., Kok, J. F., and Zhao, C.: An observationally constrained estimate of global dust aerosol optical depth, Atmos. Chem. Phys., 16, 15097–15117, https://doi.org/10.5194/acp-16-15097-2016, 2016.

Sanchez-Marroquin, A., Arnalds, O., Baustian-Dorsi, K. J., Browse, J., Dagsson-Waldhauserova, P., Harrison, A. D., Maters, E. C., Pringle, K. J., Vergara-Temprado, J., Burke, I. T., McQuaid, J. B., Carslaw, K. S., and Murray, B. J.: Iceland is an episodic source of atmospheric ice-nucleating particles relevant for mixed-phase clouds, Sci. Adv., 6, eaba8137, https://doi.org/10.1126/sciadv.aba8137, 2020.

Schill, G. P., DeMott, P. J., Emerson, E. W., Rauker, A. M. C., Kodros, J. K., Suski, K. J., Hill, T. C. J., Levin, E. J. T., Pierce, J. R., Farmer, D. K., and Kreidenweis, S. M.: The contribution of black carbon to global ice nucleating particle concentrations relevant to mixed-phase clouds, Proc Natl Acad Sci USA, 117, 22705–22711, https://doi.org/10.1073/pnas.2001674117, 2020.

Shi, Y. and Liu, X.: Dust Radiative Effects on Climate by Glaciating Mixed-Phase Clouds, Geophys. Res. Lett., 46, 6128–6137, https://doi.org/10.1029/2019GL082504, 2019.

Sirois, A. and Barrie, L. A.: Arctic lower tropospheric aerosol trends and composition at Alert, Canada: 1980–1995, 104, 11599–11618, https://doi.org/10.1029/1999JD900077, 1999.

Ullrich, R., Hoose, C., Möhler, O., Niemand, M., Wagner, R., Höhler, K., Hiranuma, N., Saathoff, H., and Leisner, T.: A New Ice Nucleation Active Site Parameterization for Desert Dust and Soot, 74, 699–717, https://doi.org/10.1175/JAS-D-16-0074.1, 2017.

Wang, Y. and Liu, X.: Immersion freezing by natural dust based on a soccer ball model with the Community Atmospheric Model version 5: climate effects, Environ. Res. Lett., 9, 124020, https://doi.org/10.1088/1748-9326/9/12/124020, 2014.

Wang, Y., Liu, X., Hoose, C., and Wang, B.: Different contact angle distributions for heterogeneous ice nucleation in the Community Atmospheric Model version 5, Atmos. Chem. Phys., 14, 10411–10430, https://doi.org/10.5194/acp-14-10411-2014, 2014.

Winker, D. M., Tackett, J. L., Getzewich, B. J., Liu, Z., Vaughan, M. A., and Rogers, R. R.: The global 3-D distribution of tropospheric aerosols as characterized by CALIOP, Atmos. Chem. Phys., 13, 3345–3361, https://doi.org/10.5194/acp-13-3345-2013, 2013.